ACS central science

http://pubs.acs.org/journal/acscii

Research Article

Activity-Based Hydrazine Probes for Protein Profiling of Electrophilic Functionality in Therapeutic Targets

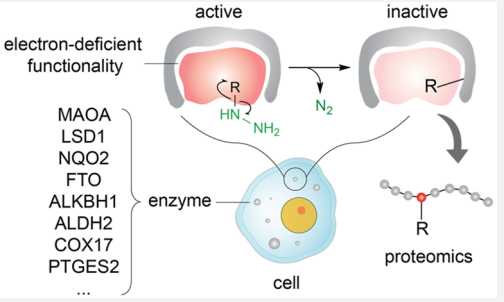
Zongtao Lin, Xie Wang, Katelyn A. Bustin, Kyosuke Shishikura, Nate R. McKnight, Lin He, Radu M. Suciu, Kai Hu, Xian Han, Mina Ahmadi, Erika J. Olson, William H. Parsons, and Megan L. Matthews*

Cite This: *ACS Cent. Sci.* 2021, 7, 1524−1534

Read Online

ACCESS | Metrics & More | Article Recommendations | Supporting Information

ABSTRACT: Most known probes for activity-based protein profiling (ABPP) use electrophilic groups that tag a single type of nucleophilic amino acid to identify cases in which its hyper-reactivity underpins function. Much important biochemistry derives from electrophilic enzyme cofactors, transient intermediates, and labile regulatory modifications, but ABPP probes for such species are underdeveloped. Here, we describe a versatile class of probes for this less charted hemisphere of the proteome. The use of an electron-rich hydrazine as the common chemical modifier enables covalent targeting of multiple, pharmacologically important classes of enzymes bearing diverse organic and inorganic cofactors. Probe attachment occurs by both polar and radicaloid mechanisms, can be blocked by molecules that occupy the active sites, and depends on the proper poise of the active site for turnover. These traits will enable the probes to be used to identify specific inhibitors of individual members of these multiple enzyme classes, making them uniquely versatile among known ABPP probes.



INTRODUCTION

Activity-based protein profiling (ABPP) was founded on the use of small, amino-acid-selective, electrophilic chemical probes to tag catalytically important residues in enzymes without steric bias from the diverse architectures of individual active sites.[1−3] The binding agnosticism of the probes allows covalent capture of entire families of enzymes, at once, while the chemical selectivity for a specific functional group (e.g., hydroxyl or thiol in serine[4,5] or cysteine hydrolases[6]) keeps the complexity of probe-labeling events manageable. Importantly, the targeting of an active site group on the basis of its functional hyper-reactivity—elicited by the specific electrostatic features of the active site—ensures that probe capture of a given enzyme can be blocked by a molecule that binds avidly in its active site, a capacity that enables discovery of specific inhibitors of the individual members within the large set initially tagged by the promiscuous probe.[7,8] This crucial capability turns the probe's lack of selectivity from vice to virtue and intimates at what could be a holy grail of ABPP—a single probe (or reactive group) that tags all enzyme active sites on the basis of a common characteristic associated with catalytic function. For electrophilic probes, the presence of multiple, different nucleophiles in essentially all enzymes would seem to preclude such generality.

By contrast to the prevalence of competent nucleophiles, reactive electrophiles are essentially absent among the common amino acids and their peptide linkages. Where present in enzymes, electrophiles are most often installed post-translationally by complex protein tailoring reactions[9,10] [e.g., pyruvoyl (Pyvl), formylglycyl (Fgly), and tyrosine quinones], incorporation of enzyme cofactors including metals,[11,12] pyridoxal 5′-phosphate,[13] flavin adenine dinucleotide (FAD),[14] and nicotinamide adenine dinucleotide (phosphate) [NAD(P)P],[15] and regulatory modifications (phosphorylation, methylation).[16] The presence of one of these moieties in a protein is not uniformly predictable from its sequence, and it is likely (i) that some are present in hitherto undiscovered locations in the proteome and (ii) that other types of electrophilic modifications remain to be discovered. Indeed, early global, unbiased screens of whole proteomes with nucleophilic hydrazine probes identified an *N*-terminal glyoxylyl (Glox) modification naturally occurring on an uncharacterized metabolic enzyme, secernin-3 (SCRN3).[10]

The set of proteins that qualified as specific hits on the basis of the stringent selection criteria imposed in this initial screen was intriguing, because it included both a small number of expected hits and a manageable number of proteins that either were not already known to possess an electrophile (e.g., SCRN3)[10] or were known to possess cofactors not expected to confer susceptibility to covalent tagging of the proteins by the

Received: May 23, 2021
Published: August 19, 2021



Downloaded via UNIV MASSACHUSETTS MEDICAL SCHOOL on February 17, 2022 at 16:19:35 (UTC).
See https://pubs.acs.org/sharingguidelines for options on how to legitimately share published articles.

ACS Publications

© 2021 The Authors. Published by American Chemical Society

https://doi.org/10.1021/acscentsci.1c00616
ACS Cent. Sci. 2021, 7, 1524−1534

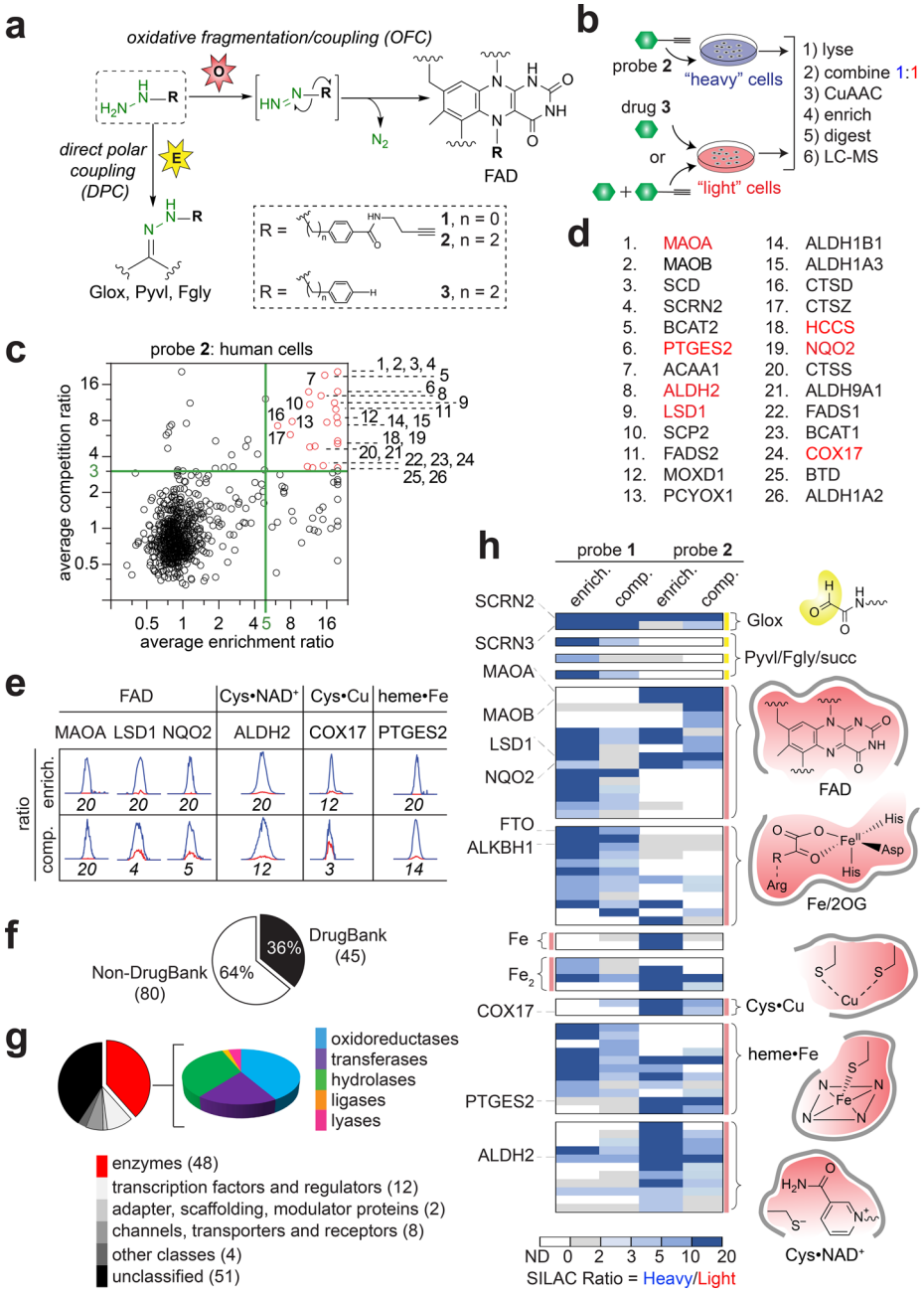


Figure 1. Substituted hydrazines broadly capture enzymes across multiple functional classes in human cells. (A) Schematic for two distinct modes of probe reactivity: direct polar coupling (DPC) and oxidative fragmentation/coupling (OFC). Green depicts the reactive probe moiety. (B) Schematic for MS1-based quantitative proteomics experiments (enrichment and competition) using stable isotopic labeling by amino acids in cell culture (SILAC). Isotopically heavy and light cells, proteomes, and peptides are depicted in blue and red, respectively. (C) Quadrant plot of average competition versus enrichment protein ratios for probe **2** from quantitative proteomic analysis of two human cell lines. (D) High-reactivity targets (enrichment ratio ≥5 and competition ratio ≥3) of probe **2**. Cofactor-dependent enzymes further investigated in this work are highlighted in red. (E) Extracted MS1 chromatograms and corresponding heavy/light ratios (enrichment and competition) for representative tryptic peptides of endogenous forms of high-reactivity targets. (F) Fraction of **2**-labeled proteins from HEK293T and MDA-MB-231 cells found in DrugBank and (G) their known or predicted functional classes. (H) Heatmap showing relative protein enrichment and competition indices for targets known or predicted to harbor electron-deficient moieties. Targets are grouped based on their type of electron-deficient group, electrophilic (yellow) or oxidizing (red) cofactor. Structures for six diverse classes (Glox, FAD, Fe/2OG, Cys·Cu, heme·Fe, and Cys·NAD$^+$) are shown (related to Figures S2−4).

hydrazine probes (e.g., enzymes with iron or noncovalent flavin cofactors).[12,17,18] In this work, we have further investigated an additional two members from the initial set of hits and six members newly identified by use of a probe modified to more closely resemble a brain-penetrant hydrazine-based drug (phenelzine).[14] As a group, the tagged proteins possess a diverse set of cofactors, initially raising concerns that they might be, in essence, false positives. To understand how the structurally and functionally disparate enzymes could all be captured—apparently specifically—by the same set of probes, we overexpressed them and determined the nature and sites of probe attachment. The results reveal two distinct, broad classes (Figure 1a) of reactivity—oxidative and polar—and distinct subclasses within the oxidative class. The chemical events

https://doi.org/10.1021/acscentsci.1c00616
ACS Cent. Sci. 2021, 7, 1524−1534

implicated suggest that the hydrazine probes are promiscuous for the different enzyme classes, because they can readily donate electrons—one or two at a time—to either directly link the hydrazine-appended clickable alkyne to the protein via an N−N bridge (direct polar coupling of DPC) or to initiate a C−N-bond fragmentation of the probe that ultimately results in attachment of its clickable alkyne substituent directly to the enzyme via C−C coupling (oxidative fragmentation/coupling, OFC). Because all the events are directed at the electron-deficient functionality in the active sites that underpin the enzymes' catalytic activities and are blocked by molecules that occupy their active sites, the probes have all the capabilities of classical ABPP probes but also an unprecedented versatility that begins to approach the single-probe holy grail that might be achievable in targeting this more sparsely populated hemisphere of the protein reactome.

RESULTS

Global Map of Hydrazine-Reactive Proteome. The initial application of the hydrazine probes was intended to identify polar electrophiles;[10] however, hits that were preliminarily identified suggested the potential for prior oxidative activation. Indeed, the hydrazine-bearing antidepressant drug phenelzine had previously been shown to undergo O_2-dependent radical chemistry to covalently inhibit its flavoenzyme target, monoamine oxidase (MAO).[14,19] To increase the likelihood that we would fully capture both modes of reactivity, we generated a global map of the hydrazine-reactive proteome with both the original broadly targeting aryl probe **1** and a chemically similar "clickable" alkylaryl hydrazine (probe **2**) that has a bond dissociation energy[20] (67 kcal/mol) less than that of phenylhydrazine (86 kcal/mol) and that more closely resembles the drug (alkylaryl hydrazine **3**) (Figure 1a).

Gel-based proteomic profiles of **2** were generated by *in situ* treatment (0.5 h, 37 °C) of HEK293T and MDA-MB-231 cells, followed by coupling of probe-captured proteins to an azide-rhodamine (Rh−N_3) reporter tag using copper(I)-catalyzed azide−alkyne cycloaddition (CuAAC or "click" chemistry)[21] and visualization by SDS−PAGE with in-gel fluorescence scanning.[1,10] Proteomic reactivity of **2** was both time- and dose-dependent, and labeling was blocked by pretreatment (15 min, 37 °C) with **3** (Figures S2−3). To identify and quantify protein targets of probe **2** *in situ*, **2**-treated cells were fractionated, conjugated by CuACC chemistry to biotin-N_3, enriched by adsorption to streptavidin resin, and analyzed by mass spectrometry (MS)-based proteomics (Figure 1b).[1,10] To quantify high-reactivity targets, proteomes from isotopically labeled[22] **2**-treated cells (1 mM, 0.5 h) were ratiometrically compared against proteomes obtained by cells subjected to two types of control treatments. To assess enrichment, cells were treated with **3** under the same conditions as **2**. To assess competition, cells were pretreated with a 10-fold excess (10 mM, 15 min) of **3** relative to **2**. This latter experiment affords estimates from the purely ratiometric quantitation of both the relative abundance of a given target and how quantitatively it is captured by the probe. Protein ratios were calculated from median peptide ratios from at least three unique quantified peptides per protein per experiment. Average competition ratios were plotted against average enrichment ratios ($n \geq 6$ biological replicates; Supplementary Data Set 1) for proteins quantified in both types of experiments (Figure 1c,d and Figure S4). Proteins that (i) were substantially enriched by the process of treatment with **2**, coupling to biotin, and absorption on streptavidin resin (ratio ≥5) and (ii) were depleted by prior treatment with **3** (ratio ≥3) in the *upper right* quadrant were taken to be high-reactivity targets (30 total proteins from the soluble and membrane fractions of the HEK293T and MDA-MB-231 cell lines). Representative peptide ratios from enrichment and competition experiments for six targets are shown in Figure 1e. Meta-analysis of expanded **2**-labeled proteins (enrichment ratio ≥5 or competition ratio ≥3) showed that, despite the facts that the competitor is an actual clinical drug and the probe is an analogue of one, the majority of targets are not found in the DrugBank (64%, Figure 1f). A large fraction of targets are known or predicted by genetics to have catalytic activity (Figure 1g, *left*). Many members of this subset are known or predicted oxidoreductases (*right*).

Capturing Enzymes across Multiple Functional Classes. As probe **2** (alkylaryl) is structurally related to **1** (aryl),[10] we aimed to understand how the target profiles compare and whether the hydrazine substituent confers selectivity. Profiles of two probes were aligned (Supplementary Data Set 2), and additional alignment of targets according to known or predicted cofactor usage (e.g., flavin, heme) or post-translational modification (PTM) generated an activity-based heatmap (Figure 1h). The two probes showed preference for SCRN3—an uncharacterized enzyme that previously provided the first example of a naturally occurring *N*-terminal glyoxylyl (Glox) electrophile. Probe **1** targeted enzymes with functional electrophilic species such as pyruvoyl (Pyvl), formylglycyl (Fgly), or succinimide (Succ),[10] whereas **1** and **2** targeted only partly overlapping sets of enzymes in other functional classes, including those defined by the use of oxidizing cofactors such as FAD, nicotinamide adenine dinucleotide (phosphate) [NAD(P)], iron (Fe), or copper (Cu). Probe **2** selectively targets MAOA and MAOB, consistent with its covalent capture of covalently bound FAD according to the known molecular mechanism of action of the phenelzine drug (**3**).[14]

The data illuminate the potential for hydrazine to serve as a general covalent modifier (and inhibitor) of enzyme targets well beyond MAO and even the flavoenzyme family. Notably, other flavoenzymes with noncovalently bound FAD cofactors [e.g., lysine-specific histone demethylase 1A (LSD1) and ribosyldihydronicotinamide dehydrogenase [quinone] (NQO2)] are also high-reactivity targets of **2**, implying that it can directly covalently couple to the enzymes themselves in addition to the FAD cofactor. Iron(II)- and 2-oxoglutarate-dependent (Fe/2OG) enzymes—including nucleic acid dioxygenase (ALKBH1) and fat mass and obesity-associated dioxygenase (FTO), the O_2-dependent RNA demethylases that are critical for an array of cellular processes and disease states, including central nervous system (CNS) function,[23] obesity,[24] and cancer[12]—were also identified as specific probe targets, with **1** being more selective than **2** toward these enzymes. To the best of our knowledge, these data are the first to show targeting of an Fe/2OG enzyme with a covalent inactivator. In addition, NAD^+-dependent aldehyde dehydrogenase (ALDH2) was a moderately selective target of probe **2**; however, covalent inhibition of alcohol metabolism enzymes by hydrazine has not previously been reported. Cu-dependent cytochrome c oxidase copper chaperone (COX17) showed selectivity toward probe **2** over **1**, suggesting a possible utility of the probes to monitor copper homeostasis and the redox state,[11] of which both are known to be disrupted in disease states.

Activity-Based Probes for Various Unexpected Classes of Enzymes. We next determined whether the broad reactivity of the hydrazine probes toward such diverse enzyme targets

https://doi.org/10.1021/acscentsci.1c00616
ACS Cent. Sci. 2021, 7, 1524−1534

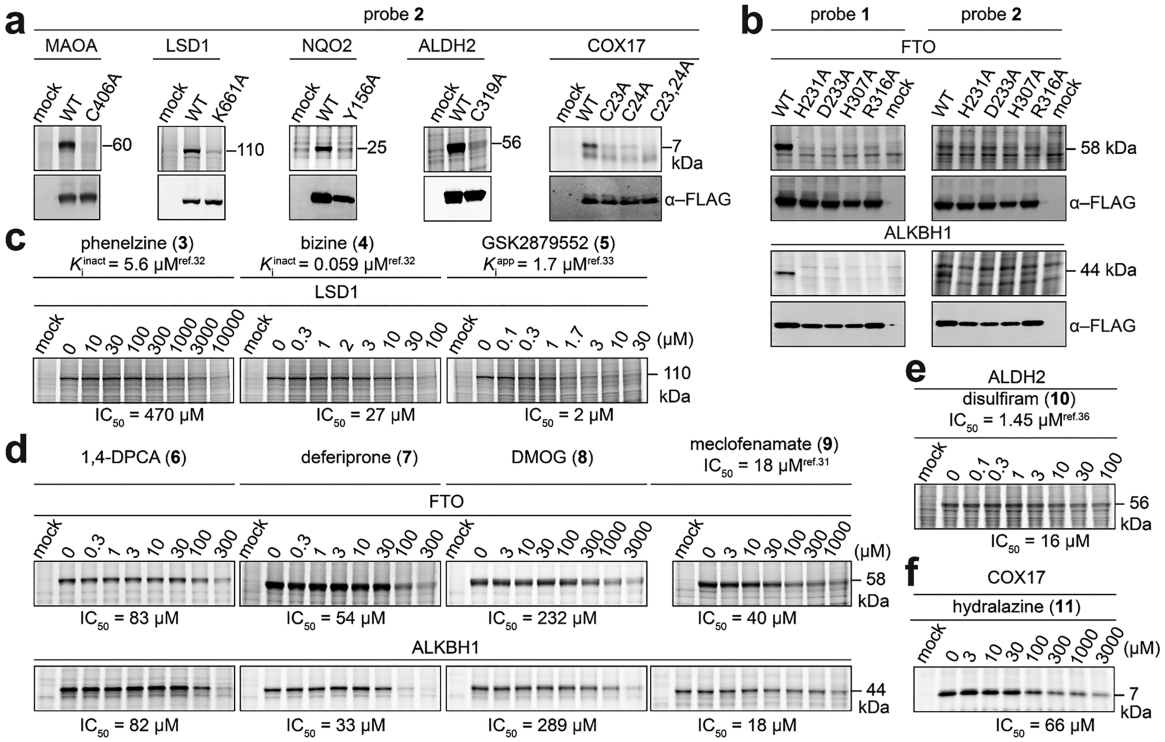


Figure 2. Covalent labeling is dependent on functional state and blocked by active-site-directed inhibitors. (A) **2**-labeling of wild-type MAOA, LSD1, NQO2, ALDH2, and COX17 but not catalytically inactive variants. Probe labeling (*upper*) and expression profiles (*lower*) for probe-treated cells overexpressing the indicated protein target or inactive variant thereof. Transfection with the appropriate empty expression vector ("mock") is used as a control. Molecular weights are indicated. (B) **1**- vs **2**-labeling of wild-type FTO and ALKBH1 but not catalytically inactive variants. Dose-dependent inhibition of (C) **1**-LSD1-labeling with covalent inhibitors phenelzine (**3**), bizine (**4**), and GSK2879552 (**5**); (D) **1**-FTO- and -ALKBH1-labeling with iron chelators [1,4-DPCA (**6**) and deferiprone (**7**)] and noncovalent inhibitors [DMOG (**8**) and meclofenamate (**9**)]; (E) **2**-ALDH2 labeling with disulfiram (**10**); (F) **2**-COX17 labeling with hydralazine, a hydrazine-containing vasodilator (**11**). Expression profiles of overexpressed wild-type enzymes were visualized by Western blot (related to Figures S5−7).

remains active-site-directed and dependent on functional state, which are the two crucial traits that have made classical ABPP probes such useful tools for inhibitor and drug discovery. These features were investigated by gel-based profiling of enzymes from six diverse structural and mechanistic classes that were robustly targeted by hydrazines: (i) covalently bound FAD-dependent monoaminergic amine oxidase A (MAOA) as a control, (ii) noncovalent flavoenzymes (epigenetic eraser LSD1 and detoxifying quinone reductase NQO2), (iii) RNA demethylases FTO and ALKBH1, (iv) alcohol-metabolizing ALDH2, (v) the Cu-binding protein COX17, and (vi) heme-binding prostaglandin E synthase 2 (PTGES2). Overexpressed wild-type proteins from probe-treated HEK293T cells retained the hydrazine reactivity and probe preference observed by proteomics analysis of their endogenous forms (Figure 2a,b). In all cases, labeling was abolished by substitution of active site residues known to be essential for activity and/or productive cofactor binding. These observations confirm that capture by the probes requires the enzymes to be in an active, functional state (Figure 2a,b).[14,25−27]

FTO and ALKBH1 are selective targets of **1**[10] but not **2** (Figures 1h and 2b), and their labeling was abolished by substitution of residues that coordinate the iron cofactor (His231, His307, and Asp233) or make key contacts with the 2OG cosubstrate (Arg316)[28,29] (Figure 2b). In addition, pretreating FTO- and ALKBH1-overexpressing HEK293T cells with the prolyl hydroxylase domain (PHD) inhibitor 1,4-DPCA (**6**), which is an iron chelator known for its anticancer[30] and regenerative activities,[31] iron chelator deferiprone (**7**), or the 2OG analogue, dimethyloxalylglycine (DMOG, **8**), all efficiently blocked probe labeling in a dose-dependent manner. Meclofenamate (**9**), a nonsteroidal, anti-inflammatory (NSAID) drug known to inhibit FTO,[32] also blocked probe labeling, and the dependence of signal abrogation on inhibitor concentration was consistent with the reported IC_{50} for binding of the drug (Figure 2d). The results suggest that, in cells, the labeling events are both active-site-directed and dependent on the presence of the cofactor. Likewise, probe labeling of LSD1 was inhibited dose-dependently by known inhibitors phenelzine (**3**),[33] bizine (**4**), and GSK2879552 (**5**). As a cyclopropylamine-containing LSD1 inhibitor with anticancer activity, **5** blocked probe labeling with an IC_{50} that is comparable to the published K_i^{app} for its target[34,35] (Figure 2c). Consistent with a hydrazine-dependent probe-labeling reaction, we report for the first time that hydralazine (**11**), an FDA-approved vasodilator that also bears a hydrazine group, blocks probe labeling of COX17 in a dose-dependent manner (Figure 2f), by unknown mechanism(s) possibly related to metal regulation.[36] The probe labeling of ALDH2 was blocked by pretreatment with disulfiram (**10**), an antialcoholism drug that covalently modifies the catalytic cysteine of ALDH2[37] (Figure 2e). Although the established targets of phenelzine, MAOA, and ALDH2 are closely related metabolic enzymes in the mitochondria, prior blockade of probe labeling of MAOA by **10** showed no effect on labeling of ALDH2 (Figure S7), suggesting that targeting of ALDH2 was independent from that of MAOA. Probe blocking by other covalent and noncovalent inhibitors and associated IC_{50} plots are shown in Figures S5−7 and Table S3. Notably,

https://doi.org/10.1021/acscentsci.1c00616
ACS Cent. Sci. 2021, 7, 1524−1534

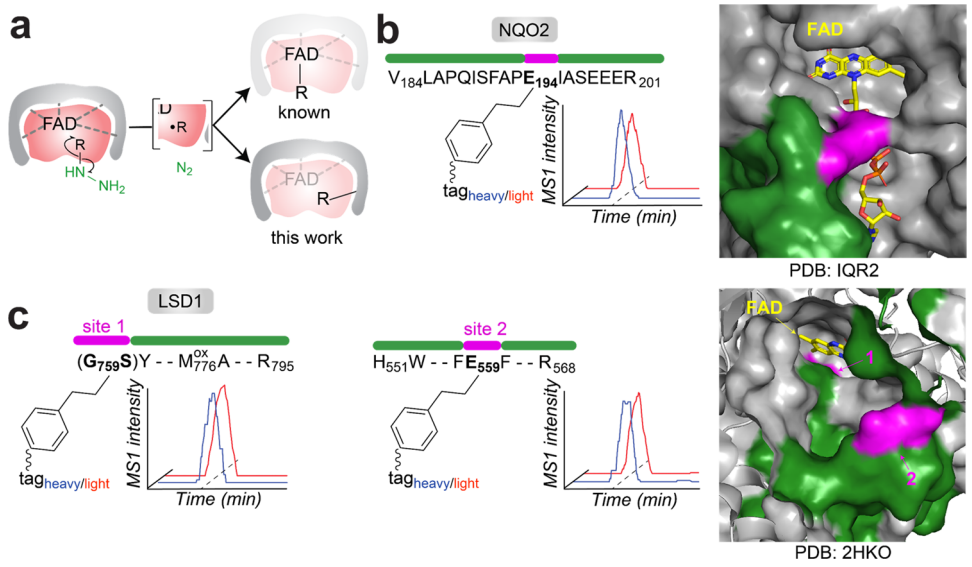


Figure 3. Covalent probes for noncovalent flavin enzymes. Identification of probe-labeling sites in NQO2 and LSD1. (A) Schematic for oxidative activation of hydrazine probes and subsequent coupling of resultant carbon-centered radical to FAD (red) and the enzyme active site (gray). Probe-labeling sites mapped onto the crystal structures of (B) NQO2 and (C) LSD1 bound to FAD (yellow). The identity of the **2**-labeled peptide and corresponding site are shown in green and magenta, respectively (*left*). Extracted MS1 ion chromatograms of coeluting heavy- and light-tagged pairs are shown in blue and red, respectively (*middle*). Probe-labeled peptides are observed as isotopic pairs due to incorporation of natural abundance (light) or $^{13}C_5{}^{15}N$ (heavy) L-valine into the portion of the tag that is retained. Peptides and sites modified in human NQO2 (PDB: IQR2) and LSD1 (PDB: 2HKO) are highlighted (*right*) (related to Figures S8−13).

pretreatment with **5** selectively inhibited probe labeling of LSD1 but did not affect that of FTO, demonstrating that the selectivity of a specific inhibitor for an individual member can be assessed across multiple enzyme families by the probe.

Mapping Sites and Mechanisms of Covalent Inactivation by Substituted Hydrazines in Living Cells. Phenelzine and related monoamine oxidase inhibitors (MAOIs) covalently target N5 of the FAD cofactor.[14] By the same mechanism, related small molecules can also inhibit other enzymes with noncovalent FAD cofactors (e.g., NQO2[17] and LSD1[18]). Reaction of **2** by the analogous mechanism (Figure 3a, *upper*) would not, in our experiments, lead to enrichment of an enzyme bearing a noncovalently bound flavin, because covalency with the protein is required for retention on the resin and detection by SDS-PAGE. Nevertheless, formation of reactive radicals, first on the nitrogen of the hydrazine moiety and, subsequently, by radical elimination of N_2 on carbon (R· in Figure 3a), could potentially result in covalent coupling directly to the protein in the vicinity of the active site (Figure 3a, *lower*). To understand the basis of the previously reported inhibition of LSD1 by phenelzine and our observation here that NQO2 is also targeted by the phenelzine-based probe, we identified the small molecule and protein products of the labeling reactions. Following reaction of either **2** or **3** with reconstituted NQO2 overexpressed in and purified from *E. coli*, FAD adducts were readily detected by LC−MS. The species observed had parent masses consistent with the loss of the N_2H_4 fragment from the probe during the coupling reaction (Figure S8). To confirm that radical coupling with the protein also occurred and that this event explains targeting of the enzymes by the probes (Figure 2a), we determined the sites of labeling using a workflow adapted from the previous study[10] (isoTOP-ABPP[38]) to enrich and identify the probe-labeled protein fragment(s) as isotopically differentiated pairs of peptides. The predominant labeling site identified in NQO2 (Figures 3b and S9) is involved in cofactor binding,[39] and the parent mass of this peptide implies a net loss of N_2H_4 in the coupling event. In addition, covalent labeling of MAOA was resolved to Trp441, an active-site residue that is adjacent to the FAD binding site (Figure S10). Similarly, we resolved the predominant site in LSD1 (site 1) down to two residues in the FAD-binding pocket that define the interface accommodating the dimethyl-isoalloxazine ring of the cofactor[40] (Figures 3c and S11). A secondary site (site 2) on the periphery of the active site was detected at much lower levels (Figures 3c and S12). For both NQO2 and LSD1, the analytical data are consistent with mechanism-based inactivation of the flavoenzymes by the hydrazine probes. The diverse labeling reactions and mass errors for all probe-labeled peptides of proteins are summarized in Figure S1 and Tables S1−2.

We observed that only probe **1** (not **2**) targeted FTO and ALKBH1 (Figures 1h and 2b). This probe selectivity contrasts with the behavior of the FAD-harboring enzymes and suggests a distinct mechanism of probe capture for the Fe/2OG enzymes. It also establishes that relatively subtle details of structure can tune probes to be either more promiscuous or more selective with respect to different functional classes. Here, iron-hydrazine coordination may be an initial step, as hydrazide- and hydroxylamine-containing compounds have been shown to inhibit FTO[41] by binding noncovalently to the iron center. However, to our knowledge, hydrazine reactivity leading to covalent enzyme modification has not yet been reported for a member of the Fe/2OG enzyme class. To define the mode of reactivity (DPC or OFC, Figure 1a), we used ^{15}N-isotopologues of **1** to capture FTO from overexpressing HEK293T cells (Figure 4a). SCRN3 was used as a control for DPC (Figures 4b and S14). Peptide pairs from both data sets were filtered according to retention time, parent mass, MS1 intensity, and sample specificity (Supplementary Data Set 3). This analysis yielded only ^{15}N-insensitive pairs (three) from the FTO data set, suggesting a loss of at least the terminal nitrogen atom from the probe during coupling to the Fe/2OG enzyme (Figure S15). Next, the experimental MS2 spectra of the most abundant pair

https://doi.org/10.1021/acscentsci.1c00616
ACS Cent. Sci. 2021, 7, 1524−1534

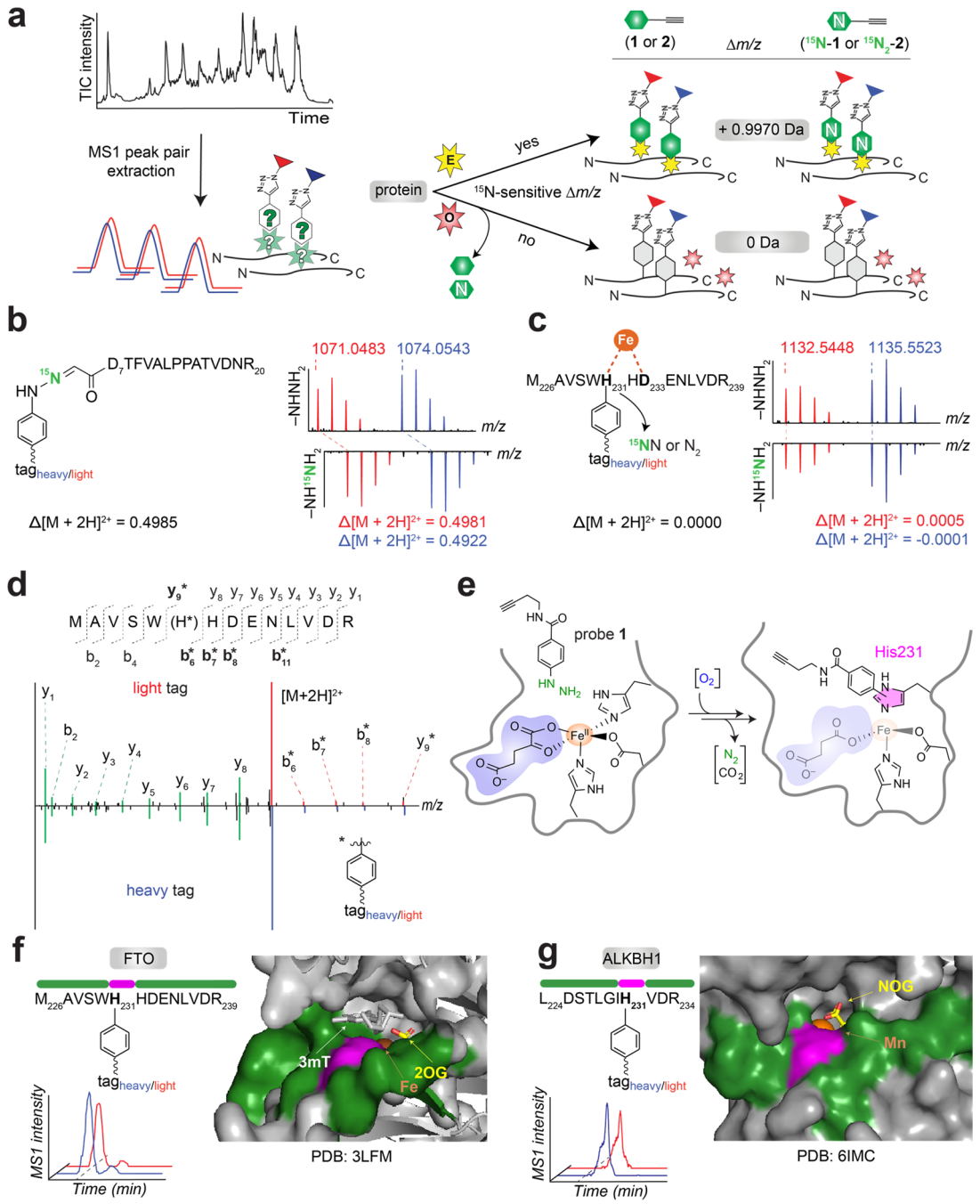


Figure 4. Discovery of a covalent inactivator of FTO, ALKBH1, and other Fe/2OG enzymes. (A) Experimental strategy to determine site(s) of covalent modification and mode(s) of probe reactivity with isotopic hydrazine probes. MS1 pairs of probe-labeled peptides arising from the tags are identified independently of their mass or sequence (*left*). OFC and DPC manifolds of the peptide pairs are then differentiated according to whether the parent mass changes upon use of the ^{15}N-labeled probe (*right*). In pairs that shift 0.9970 Da, the hydrazine group is retained (DPC manifold); in pairs that do not shift, the hydrazine group is lost (OFC manifold). Probe-labeling schemes (*left*) and corresponding isotopic envelopes (*right*) of peptide pairs isolated from (B) SCRN3-transfected or (C) FTO-transfected cells treated with **1** versus **^{15}N-1**. (D) Comparison of high-resolution MS2 spectra generated from light- versus heavy-tagged parent ions for the FTO peptide pair in C. (E) Schematic for enzyme activation of probe **1** in a radical manifold, resulting in arylation of the active site His side chain that coordinates the iron center. The hydrazine moiety, 2OG, and iron are shown in green, blue, and brown, respectively. Probe-labeled peptides and sites of modification mapped onto (F) FTO and (G) ALKBH1 crystal structures. The identity of the **1**-labeled peptides (aa 226−239 and 224−234 for FTO and ALKBH1, respectively) and site (H231) are shown in green and magenta, respectively (*left*). Extracted MS1 ion chromatograms of coeluting heavy- and light-tagged peptides are shown in blue and red, respectively (*middle*). Modified peptides are highlighted in the FTO (PDB: 3LFM) and ALKBH1 (PDB: 6IMC) active site structures (*right*). Iron (brown), 2OG (yellow), and FTO substrate 3-methylthymine (gray) are highlighted (related to Figures S13−17).

were searched against theoretical MS2 spectra for all possible peptide assignments of FTO. Using this approach, the predominant site of probe capture could be unambiguously assigned to His231 (Figures 4c,d and S15−16), one of the three cofactor ligands.[28,29] The mass of the peptide and corresponding ^{15}N-insensitivity are consistent with the OFC mechanism

https://doi.org/10.1021/acscentsci.1c00616
ACS Cent. Sci. 2021, 7, 1524−1534

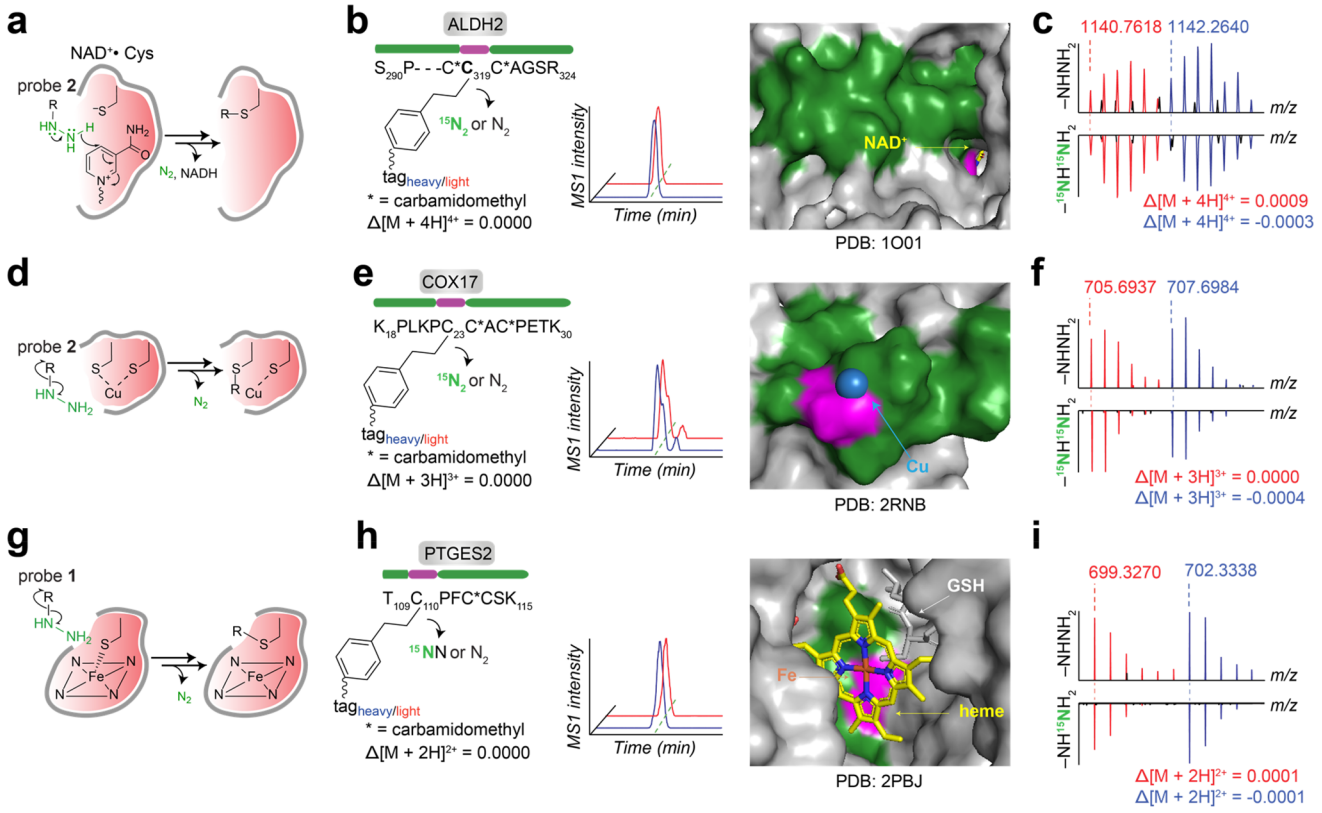


Figure 5. Covalent modification of active site cysteine residues in ALDH2, COX17, and PTGES2. Schematic for enzyme activation of hydrazine probes and subsequent alkylation of catalytic and cofactor-binding cysteine residues in (A) ALDH2, (D) COX17, and (G) PTGES2, respectively. Probe-labeled peptides and sites of modification mapped onto (B) ALDH2 bound to NAD^+ (yellow), (E) COX17 bound to copper (blue), and (H) PTGES2 bound to heme iron (yellow) crystal structures. The identity of the probe-labeled peptides (aa 290−324, 18−30, and 109−115, respectively) and sites (C319, C23, and C110, respectively) are shown in green and magenta, respectively (*left*). Extracted MS1 ion chromatograms of coeluting heavy- and light-tagged peptides are shown in blue and red, respectively. Modified peptides are highlighted in the human ALDH2 (PDB: 1O01, human), COX17 (PDB: 6IMC, human), and PTGES2 (PDB: 2PBJ, monkey) active site structures (*right*). Comparison of MS1 isotopic envelopes of cysteine-labeled peptide pairs isolated from (C) ALDH2-, (F) COX17-, and (I) PTGES2-transfected cells treated with **2** (or **1**) versus $^{15}N_2$-**2** (or ^{15}N-**1**) (related to Figures S18, S19, and S22).

(Figure 1a) that involves enzyme activation of the probe in a radical manifold that results in arylation of the His-coordinated side chain with loss of N_2 (Figure 4e). As can be seen from the crystal structure of FTO with a bound nucleic acid substrate, His arylation should almost certainly disrupt binding of the substrate, 2OG cosubstrate, and/or the iron cofactor (Figure 4f). The covalent labeling of ALKBH1 at iron ligand His231 was also observed (Figures 4g and S17). The data show that hydrazines define a new class of mechanism-based inactivators for Fe/2OG enzymes. In addition, we identified 13 other members of the Fe/2OG family belonging to separate sequence clades and functional classes as high-reactivity probe targets (Figures 1h and S13), suggesting that the labeling mechanism is likely to be general.

ALDH2, the second enzyme to metabolize alcohol, primarily catalyzes the NAD^+-dependent oxidation of aldehydes to generate the corresponding carboxylic acids, and it is also known to form covalent adducts when presented with noncanonical substrates or inhibitors.[15,42,43] However, covalent inhibition of alcohol metabolism enzymes by hydrazine has not previously been reported. To elucidate the basis for probe labeling of ALDH2 by hydrazines, we applied the same method used for the flavoenzymes above. Processed proteomes from **2**-treated ALDH2-transfected HEK293T cells were analyzed by LC−MS/MS. The data revealed a **2**-labeled peptide at the catalytic cysteine residue (Cys319) with a loss of N_2H_4 (Figure 5a,b). Labeling of ALDH2 by isotopic probes (**2** and $^{15}N_2$-**2**) yielded the same MS1 isotopic envelopes of the modified peptide (Figure 5c), suggesting a structural transformation of the probe that involved the loss of the hydrazine group (Figure S18). Modification of the catalytic cysteine suggests either direct reaction with organohydrazines or an activated derivative thereof, consistent with the diminished labeling in C-to-A variant proteins (Figure 2a) and mechanism-based inactivation of ALDH2 by Cys alkylation in the literature.[15,42,43] As administration of phenelzine is known to exacerbate the toxicity of alcohol consumption in patients, our results on ALDH2 may provide a potential inhibition mechanism to explain this clinically observed drug−food interaction. Phylogenetic analysis of the family shows that 9 out of 19 ALDH isozymes are hydrazine targets (Figure S13), suggesting that the covalent inhibition of ALDH2 activity may also explain the labeling mechanisms of other NAD^+-dependent enzymes.

As a copper chaperone,[11] COX17 delivers copper ions to the mitochondria for cytochrome c oxidase activation. It is a known anticancer target[11] that is relatively understudied, as no targeting approach or developed small molecule modulators have been made available to date. Our profiling data provide the first indication that COX17 could be covalently targeted by hydrazines (Figure 1). Modification of individual catalytic

https://doi.org/10.1021/acscentsci.1c00616
ACS Cent. Sci. 2021, 7, 1524−1534

cysteines showed significantly decreased probe labeling activity, whereas the C23,24A double-variant lost activity completely, suggesting that probe reactivity is dependent on the functional state of the Cu-binding site (Figure 2a). In addition, COX17 labeling was not effectively blocked by thiol-alkylating electrophiles, as high concentrations of iodoacetamide (100−200 μM) only partially reduced probe labeling in living cells and lysates (Figure S20). The modest reactivity of these cysteines is consistent with that of metal-bound thiolates reported in the literature[6,38,44] and suggests that the probes are specific for the Cu-bound form. Similar to ALDH2, COX17 yielded a **2**-labeled peptide at Cys23 with a net loss of N_2H_4 (Figures 5d,e and S19). Isotopic probes (**2** and $^{15}\mathbf{N_2}$-**2**) showed the same MS1 envelopes (Figure 5f), confirming the loss of hydrazine by the OFC reaction manifold (Figure 1a). Cys23 and Cys24 both ligate the Cu ion in human COX17; however, our data showed a preference for Cys23 as the labeled site. As covalent modification of Cys23 would significantly disrupt Cu binding (Figure 5e), hydrazines may serve as a tool for evaluating copper homeostasis in cells.

Heme enzymes, known to react with hydrazine and form alkylated heme products,[45,46] represent an additional class of highly reactive targets of the hydrazine probes (Figure 1h). Three targets including full-length and truncated prostaglandin E synthase 2 (PTGES2), holocytochrome c-type synthase (HCCS), and heme oxygenase 2 (HMOX2) were covalently labeled by the hydrazine probes (Figure S21), suggesting that alkylation of protein side chains may have occurred in addition to alkylation of the heme cofactor. Probes **1** and **2** displayed comparable labeling reactivities with PTGES2 and HMOX2; however, **1** and **2** selectively labeled truncated PTGES2 and HCCS, respectively (Figure S21). In our effort to resolve the labeling site in truncated PTGES2, we identified **1**-labeled Cys110 with a loss of hydrazine (Figures 5g,h and S22). The OFC reaction mode was confirmed by the use of isotopic probes (**1** and $^{15}\mathbf{N}$-**1**), yielding the same MS1 isotopic envelopes for the modified peptide (Figure 5i). Cys110 is a critical residue in PTGES2, as the C110S mutation has been shown to abolish catalytic activity.[47,48] As such, covalent modification of this residue by the hydrazine probe would also be expected to disrupt the active site and result in a loss of catalytic activity (Figure 5h). As the labeling mechanism of PTGES2 is expected to be conserved for other heme targets, our data may suggest an effective avenue for covalent targeting of heme-dependent enzymes.

In addition to enzymes with elucidated sites of probe labeling, other functional classes of proteins are covalently reactive toward the hydrazine probe in human cells (Supplementary Data Sets 1 and 2 and Figure 1h). For example, 2-aminoethanethiol dioxygenase (ADO), known or predicted to require Fe, showed reactivity and covalent bond formation with hydrazine (Figure 1h). Representative peptide ratios from enrichment and competition experiments and covalent labeling by probes **1** and **2** of wild-type proteins overexpressed in HEK293T cells are shown in Figure S23. Although the labeling sites and mechanisms of many targets have yet to be elucidated, we expect that at least a subset of these will form in a cofactor-dependent and active-site-directed manner, consistent with the above-mentioned classes of enzymes. Currently, there are no inhibitors available for most of these cofactor-dependent enzymes, and their physiological functions are incompletely understood. Further investigation of modified sites and reactivities could potentially uncover probe-labeling mechanisms that define new enzymatic activities, and, importantly, convert small molecule leads into inhibitor/drug candidates that selectively modulate, covalently or noncovalently, enzymes from remarkably diverse functional classes.

DISCUSSION

We have shown here that hydrazine probes modify different classes of enzymes that share only the property of functional electron deficiency (Figure 1). The probes are mechanism-based and active-site-directed, and they report on the occupancy of active sites by specific binders. These features are the basis for ABPP and its capacity to discover enzymes, inhibitors, and drugs.[1−3] The results show that ABPP probes can dispense with not only the specific molecular recognition by an enzyme active site but also the chemical selectivity that has characterized electrophilic ABPP probes for functional nucleophiles, by far the predominant use of the method to date. As such, this work represents a step toward the ultimate objective of a single probe that tags enzymes on the basis of a conserved trait associated with catalytic function.

As our ABPP approach for evaluating cofactor-dependent enzyme biochemistry may facilitate new areas of therapeutic development, we assessed the utility of hydrazine probes to identify and evaluate specific inhibitors in living cells and independent of substrates (Figures 2 and S5). A set of 13 commercially available inhibitors and drugs were screened for their ability to block probe labeling of at least one of eight total enzyme targets found in six distinct cofactor classes. The data demonstrate that the probes can both identify unknown targets of these inhibitors and measure their potency and selectivity across the hydrazine-sensitive proteome. Inhibitors operating by a variety of mechanisms can be evaluated, as covalent (both reversible and irreversible) modifiers and noncovalent binders could be quantified. The hydrazine probes themselves may also represent their own starting points to explore both DPC and OFC reaction manifolds (Figure 1a) for their ability to be made more selective, either for reaction type, cofactor class, or potentially even individual members within a given enzyme family. Following the many successful examples of amino-acid-targeting enzyme inhibitors, the next phase will be to elaborate and tune hydrazines for specific cofactor classes and reaction modes to explore whether diversified nucleophiles have the same capacity as electrophiles to serve as potent and selective inhibitors of cofactor-dependent enzymes.

This approach may be particularly useful for evaluating inhibitors for Fe/2OG enzymes, as they are a large and diverse enzyme class that has not been well targeted for drug therapies.[12,23,24] Most known inhibitors target the 2OG binding site or chelate the iron cofactor.[12,49] As both design strategies disrupt catalytic features conserved across the family, they are poorly selective and not specific for the active state. Here, probe labeling occurs by covalent inactivation in an iron-, 2OG-, and likely O_2-dependent manner and is blocked by inhibitors occupying active sites with high selectivity for their primary substrates (Figure 4). Therefore, organohydrazines represent an entrée into probing for molecules that block such functional hotspots expected to be more amenable to the development of selective inhibitors. Overall, we expect hydrazine probes to retain all the capabilities of classical ABPP probes, including the discovery of inhibitors and new mechanisms of action.

Hydrazine drugs like phenelzine have long been regarded as poor drugs, owing to their chemical promiscuity, which caused unwanted side effects in patients. However, in all cases we

https://doi.org/10.1021/acscentsci.1c00616
ACS Cent. Sci. 2021, 7, 1524−1534

investigated to date, target promiscuity is active-site-directed and mechanism-based. Such versatility of hydrazine-containing drugs may indicate their potential to be repurposed and/or optimized for the treatment of other CNS diseases. Indeed, phenelzine is known to have antiaddictive effects,[50,51] and MAOIs have reported efficacy for fibromyalgia,[52] pain,[53] bipolar disorder,[54] Parkinson's disease,[55] and multiple-system atrophy.[56] Taken together, these facts indicate that MAOIs and their targets have druggable potential for a broad spectrum of brain diseases. Guided by the principles of ABPP, organohydrazines may serve as a broadly useful pharmacophore to explore target−phenotype relationships.

■ ASSOCIATED CONTENT

Supporting Information

The Supporting Information is available free of charge at https://pubs.acs.org/doi/10.1021/acscentsci.1c00616.

Tables S1−3; Figures S1−23; supplementary biological and synthetic methods; custom codes and scripts (PDF)

Supplementary Data Set 1. Compiled proteomics data (XLSX)

Supplementary Data Set 2. Protein targets comparison between probes (XLSX)

Supplementary Data Set 3. Characterization of probe-labeling site on FTO (XLSX)

■ AUTHOR INFORMATION

Corresponding Author

Megan L. Matthews − *Department of Chemistry, University of Pennsylvania, Philadelphia, Pennsylvania 19104, United States;* orcid.org/0000-0003-1178-4616; Email: megamatt@sas.upenn.edu

Authors

Zongtao Lin − *Department of Chemistry, University of Pennsylvania, Philadelphia, Pennsylvania 19104, United States*

Xie Wang − *Department of Chemistry, University of Pennsylvania, Philadelphia, Pennsylvania 19104, United States;* orcid.org/0000-0002-7292-5550

Katelyn A. Bustin − *Department of Chemistry, University of Pennsylvania, Philadelphia, Pennsylvania 19104, United States;* orcid.org/0000-0001-8933-9825

Kyosuke Shishikura − *Department of Chemistry, University of Pennsylvania, Philadelphia, Pennsylvania 19104, United States*

Nate R. McKnight − *Department of Chemistry, University of Pennsylvania, Philadelphia, Pennsylvania 19104, United States*

Lin He − *Zenagem, LLC, Fountain Valley, California 92708, United States;* orcid.org/0000-0003-4945-2107

Radu M. Suciu − *Department of Chemistry, The Scripps Research Institute, La Jolla, California 92037, United States*

Kai Hu − *Department of Molecular, Cell and Cancer Biology, University of Massachusetts Medical School, Worcester, Massachusetts 01605, United States*

Xian Han − *Department of Structural Biology, St. Jude Children's Research Hospital, Memphis, Tennessee 38105, United States*

Mina Ahmadi − *Department of Chemistry, University of Pennsylvania, Philadelphia, Pennsylvania 19104, United States*

Erika J. Olson − *Department of Chemistry, The Scripps Research Institute, La Jolla, California 92037, United States*

William H. Parsons − *Department of Chemistry and Biochemistry, Oberlin College, Oberlin, Ohio 44074, United States;* orcid.org/0000-0001-6065-2340

Complete contact information is available at: https://pubs.acs.org/10.1021/acscentsci.1c00616

Author Contributions

Z.L. and M.L.M. designed the experiments, analyzed data, and wrote the manuscript. Z.L. developed methods and performed experiments. X.W. and W.H.P. synthesized probes. Z.L. and K.A.B. performed site of labeling experiments. N.R.M., K.S., and M.A. performed cloning and gel-based ABPP experiments. L.H. developed Java scripts to analyze data. R.M.S. managed CIMAGE software. X.H. developed R scripts for meta-analysis. K.H. generated dendrograms of targeted enzyme families. E.J.O. and M.L.M. synthesized isotopic biotin azide peptide tags for site of labeling experiments. All authors revised the manuscript.

Notes

The authors declare the following competing financial interest(s): M.L.M. is a founder, shareholder and scientific adviser to Zenagem, LLC.

■ ACKNOWLEDGMENTS

This work was supported by the University of Pennsylvania (M.L.M.), Oberlin College (W.H.P.), National Institutes of Health NIDA 1DP1DA051620 (M.L.M.), NIGMS 5T32GM071339-15 (K.A.B.), American Cancer Society 129784-IRG-16-188-38-IRG (M.L.M.), and Astellas Foundation for Research on Metabolic Disorders (K.S.). The authors are grateful for the computational support from Simone Sidoli (Albert Einstein College of Medicine), Tammer Ibrahim, Hee Jong Kim, and Benjamin A. Garcia (University of Pennsylvania), Robin Park (Integrated Proteomics Applications, Inc.), Benjamin F. Cravatt (The Scripps Research Institute), and Junmin Peng (St. Jude Children's Research Hospital). We thank Sara M. Martin and Victor Khong (M.L.M. group) for their assistance with cloning, Ellen Heber-Katz (Lankenau Institute for Medical Research) for providing 1,4-DPCA, Bin Yu (Zhengzhou University) for providing LSD1 inhibitors, Philip E. Dawson (The Scripps Research Institute) for assistance with TEV tag preparation, and J. Martin Bollinger Jr. (Pennsylvania State University) for helpful discussions and editorial assistance.

■ REFERENCES

(1) Niphakis, M. J.; Cravatt, B. F. Enzyme inhibitor discovery by activity-based protein profiling. *Annu. Rev. Biochem.* **2014**, *83*, 341−77.

(2) Jones, L. H.; Neubert, H. Clinical chemoproteomics-opportunities and obstacles. *Sci. Transl. Med.* **2017**, *9* (386), eaaf7951.

(3) Drewes, G.; Knapp, S. Chemoproteomics and chemical probes for target discovery. *Trends Biotechnol.* **2018**, *36* (12), 1275−1286.

(4) Bachovchin, D. A.; Cravatt, B. F. The pharmacological landscape and therapeutic potential of serine hydrolases. *Nat. Rev. Drug Discovery* **2012**, *11* (1), 52−68.

(5) Kok, B. P.; Ghimire, S.; Kim, W.; Chatterjee, S.; Johns, T.; Kitamura, S.; Eberhardt, J.; Ogasawara, D.; Xu, J.; Sukiasyan, A.; Kim, S. M.; Godio, C.; Bittencourt, J. M.; Cameron, M.; Galmozzi, A.; Forli, S.; Wolan, D. W.; Cravatt, B. F.; Boger, D. L.; Saez, E. Discovery of small-molecule enzyme activators by activity-based protein profiling. *Nat. Chem. Biol.* **2020**, *16* (9), 997−1005.

(6) Backus, K. M.; Correia, B. E.; Lum, K. M.; Forli, S.; Horning, B. D.; González-Páez, G. E.; Chatterjee, S.; Lanning, B. R.; Teijaro, J. R.;

Olson, A. J.; Wolan, D. W.; Cravatt, B. F. Proteome-wide covalent ligand discovery in native biological systems. *Nature* **2016**, *534* (7608), 570.
(7) Vinogradova, E. V.; Zhang, X.; Remillard, D.; Lazar, D. C.; Suciu, R. M.; Wang, Y.; Bianco, G.; Yamashita, Y.; Crowley, V. M.; Schafroth, M. A.; Yokoyama, M.; Konrad, D. B.; Lum, K. M.; Simon, G. M.; Kemper, E. K.; Lazear, M. R.; Yin, S.; Blewett, M. M.; Dix, M. M.; Nguyen, N.; Shokhirev, M. N.; Chin, E. N.; Lairson, L. L.; Melillo, B.; Schreiber, S. L.; Forli, S.; Teijaro, J. R.; Cravatt, B. F. An Activity-Guided Map of Electrophile-Cysteine Interactions in Primary Human T Cells. *Cell* **2020**, *182* (4), 1009−1026.e29.
(8) Hacker, S. M.; Backus, K. M.; Lazear, M. R.; Forli, S.; Correia, B. E.; Cravatt, B. F. Global profiling of lysine reactivity and ligandability in the human proteome. *Nat. Chem.* **2017**, *9* (12), 1181−1190.
(9) Walsh, C. T. *Posttranslational modification of proteins: expanding nature's inventory*; Roberts and Company Publishers: Greenwood Village, 2006.
(10) Matthews, M. L.; He, L.; Horning, B. D.; Olson, E. J.; Correia, B. E.; Yates, J. R., 3rd; Dawson, P. E.; Cravatt, B. F. Chemoproteomic profiling and discovery of protein electrophiles in human cells. *Nat. Chem.* **2017**, *9* (3), 234−243.
(11) Suzuki, C.; Daigo, Y.; Kikuchi, T.; Katagiri, T.; Nakamura, Y. Identification of COX17 as a therapeutic target for non-small cell lung cancer. *Cancer Res.* **2003**, *63* (21), 7038.
(12) Huang, Y.; Su, R.; Sheng, Y.; Dong, L.; Dong, Z.; Xu, H.; Ni, T.; Zhang, Z. S.; Zhang, T.; Li, C.; Han, L.; Zhu, Z.; Lian, F.; Wei, J.; Deng, Q.; Wang, Y.; Wunderlich, M.; Gao, Z.; Pan, G.; Zhong, D.; Zhou, H.; Zhang, N.; Gan, J.; Jiang, H.; Mulloy, J. C.; Qian, Z.; Chen, J.; Yang, C. G. Small-molecule targeting of oncogenic FTO demethylase in acute myeloid leukemia. *Cancer Cell* **2019**, *35* (4), 677−691.e10.
(13) Liang, J.; Han, Q.; Tan, Y.; Ding, H.; Li, J. Current Advances on Structure-Function Relationships of Pyridoxal 5′-Phosphate-Dependent Enzymes. *Front Mol. Biosci* **2019**, *6*, 4.
(14) Binda, C.; Wang, J.; Li, M.; Hubalek, F.; Mattevi, A.; Edmondson, D. E. Structural and mechanistic studies of arylalkylhydrazine inhibition of human monoamine oxidases A and B. *Biochemistry* **2008**, *47* (20), 5616−25.
(15) Khanna, M.; Chen, C. H.; Kimble-Hill, A.; Parajuli, B.; Perez-Miller, S.; Baskaran, S.; Kim, J.; Dria, K.; Vasiliou, V.; Mochly-Rosen, D.; Hurley, T. D. Discovery of a novel class of covalent inhibitor for aldehyde dehydrogenases. *J. Biol. Chem.* **2011**, *286* (50), 43486−94.
(16) Zhou, W.; Deiters, A. Chemogenetic and optogenetic control of post-translational modifications through genetic code expansion. *Curr. Opin. Chem. Biol.* **2021**, *63*, 123−131.
(17) Yan, C.; Dufour, M.; Siegel, D.; Reigan, P.; Gomez, J.; Shieh, B.; Moody, C. J.; Ross, D. Indolequinone inhibitors of NRH:quinone oxidoreductase 2. Characterization of the mechanism of inhibition in both cell-free and cellular systems. *Biochemistry* **2011**, *50* (31), 6678−88.
(18) Culhane, J. C.; Wang, D.; Yen, P. M.; Cole, P. A. Comparative analysis of small molecules and histone substrate analogues as LSD1 lysine demethylase inhibitors. *J. Am. Chem. Soc.* **2010**, *132* (9), 3164−76.
(19) Polasek, T. M.; Elliot, D. J.; Somogyi, A. A.; Gillam, E. M.; Lewis, B. C.; Miners, J. O. An evaluation of potential mechanism-based inactivation of human drug metabolizing cytochromes P450 by monoamine oxidase inhibitors, including isoniazid. *Br. J. Clin. Pharmacol.* **2006**, *61* (5), 570−84.
(20) St. John, P. C.; Guan, Y.; Kim, Y.; Kim, S.; Paton, R. S. Prediction of organic homolytic bond dissociation enthalpies at near chemical accuracy with sub-second computational cost. *Nat. Commun.* **2020**, *11* (1), 2328.
(21) Rostovtsev, V. V.; Green, L. G.; Fokin, V. V.; Sharpless, K. B. A stepwise huisgen cycloaddition process: copper(I)-catalyzed regioselective "ligation" of azides and terminal alkynes. *Angew. Chem., Int. Ed.* **2002**, *41* (14), 2596−9.
(22) Ong, S. E.; Blagoev, B.; Kratchmarova, I.; Kristensen, D. B.; Steen, H.; Pandey, A.; Mann, M. Stable isotope labeling by amino acids in cell culture, SILAC, as a simple and accurate approach to expression proteomics. *Mol. Cell Proteomics* **2002**, *1* (5), 376−86.
(23) Hess, M. E.; Hess, S.; Meyer, K. D.; Verhagen, L. A.; Koch, L.; Bronneke, H. S.; Dietrich, M. O.; Jordan, S. D.; Saletore, Y.; Elemento, O.; Belgardt, B. F.; Franz, T.; Horvath, T. L.; Ruther, U.; Jaffrey, S. R.; Kloppenburg, P.; Bruning, J. C. The fat mass and obesity associated gene (Fto) regulates activity of the dopaminergic midbrain circuitry. *Nat. Neurosci.* **2013**, *16* (8), 1042−8.
(24) Claussnitzer, M.; Dankel, S. N.; Kim, K. H.; Quon, G.; Meuleman, W.; Haugen, C.; Glunk, V.; Sousa, I. S.; Beaudry, J. L.; Puviindran, V.; Abdennur, N. A.; Liu, J.; Svensson, P. A.; Hsu, Y. H.; Drucker, D. J.; Mellgren, G.; Hui, C. C.; Hauner, H.; Kellis, M. FTO obesity variant circuitry and adipocyte browning in humans. *N. Engl. J. Med.* **2015**, *373* (10), 895−907.
(25) Wu, H. F.; Chen, K.; Shih, J. C. Site-directed mutagenesis of monoamine oxidase A and B: role of cysteines. *Mol. Pharmacol.* **1993**, *43* (6), 888.
(26) Karasulu, B.; Patil, M.; Thiel, W. Amine oxidation mediated by lysine-specific demethylase 1: quantum mechanics/molecular mechanics insights into mechanism and role of lysine 661. *J. Am. Chem. Soc.* **2013**, *135* (36), 13400−13.
(27) Xu, J.; Patrick, B. A.; Jaiswal, A. K. NRH:quinone oxidoreductase 2 (NQO2) protein competes with the 20 S proteasome to stabilize transcription factor CCAAT enhancer-binding protein alpha (C/EBPalpha), leading to protection against gamma radiation-induced myeloproliferative disease. *J. Biol. Chem.* **2013**, *288* (48), 34799−808.
(28) Han, Z.; Niu, T.; Chang, J.; Lei, X.; Zhao, M.; Wang, Q.; Cheng, W.; Wang, J.; Feng, Y.; Chai, J. Crystal structure of the FTO protein reveals basis for its substrate specificity. *Nature* **2010**, *464* (7292), 1205−9.
(29) Jia, G.; Fu, Y.; Zhao, X.; Dai, Q.; Zheng, G.; Yang, Y.; Yi, C.; Lindahl, T.; Pan, T.; Yang, Y. G.; He, C. N6-methyladenosine in nuclear RNA is a major substrate of the obesity-associated FTO. *Nat. Chem. Biol.* **2011**, *7* (12), 885−7.
(30) Xiong, G.; Deng, L.; Zhu, J.; Rychahou, P. G.; Xu, R. Prolyl-4-hydroxylase alpha subunit 2 promotes breast cancer progression and metastasis by regulating collagen deposition. *BMC Cancer* **2014**, *14* (1), 1.
(31) Zhang, Y.; Strehin, I.; Bedelbaeva, K.; Gourevitch, D.; Clark, L.; Leferovich, J.; Messersmith, P. B.; Heber-Katz, E. Drug-induced regeneration in adult mice. *Sci. Transl. Med.* **2015**, *7* (290), 290ra92.
(32) Huang, Y.; Yan, J.; Li, Q.; Li, J.; Gong, S.; Zhou, H.; Gan, J.; Jiang, H.; Jia, G. F.; Luo, C.; Yang, C. G. Meclofenamic acid selectively inhibits FTO demethylation of m6A over ALKBH5. *Nucleic Acids Res.* **2015**, *43* (1), 373−84.
(33) Prusevich, P.; Kalin, J. H.; Ming, S. A.; Basso, M.; Givens, J.; Li, X.; Hu, J.; Taylor, M. S.; Cieniewicz, A. M.; Hsiao, P.-Y.; et al. A selective phenelzine analogue inhibitor of histone demethylase LSD1. *ACS Chem. Biol.* **2014**, *9* (6), 1284−1293.
(34) Mohammad, H. P.; Smitheman, K. N.; Kamat, C. D.; Soong, D.; Federowicz, K. E.; Van Aller, G. S.; Schneck, J. L.; Carson, J. D.; Liu, Y.; Butticello, M.; Bonnette, W. G.; Gorman, S. A.; Degenhardt, Y.; Bai, Y.; McCabe, M. T.; Pappalardi, M. B.; Kasparec, J.; Tian, X.; McNulty, K. C.; Rouse, M.; McDevitt, P.; Ho, T.; Crouthamel, M.; Hart, T. K.; Concha, N. O.; McHugh, C. F.; Miller, W. H.; Dhanak, D.; Tummino, P. J.; Carpenter, C. L.; Johnson, N. W.; Hann, C. L.; Kruger, R. G. A DNA hypomethylation signature predicts antitumor activity of LSD1 inhibitors in SCLC. *Cancer Cell* **2015**, *28* (1), 57−69.
(35) Tan, A. H. Y.; Tu, W.; McCuaig, R.; Hardy, K.; Donovan, T.; Tsimbalyuk, S.; Forwood, J. K.; Rao, S. Lysine-specific histone demethylase 1A regulates macrophage polarization and checkpoint molecules in the tumor microenvironment of triple-negative breast cancer. *Front. Immunol.* **2019**, *10*, 1351.
(36) Knowles, H. J.; Tian, Y. M.; Mole, D. R.; Harris, A. L. Novel mechanism of action for hydralazine: induction of hypoxia-inducible factor-1alpha, vascular endothelial growth factor, and angiogenesis by inhibition of prolyl hydroxylases. *Circ. Res.* **2004**, *95* (2), 162−9.
(37) Lam, J. P.; Mays, D. C.; Lipsky, J. J. Inhibition of Recombinant Human Mitochondrial and Cytosolic Aldehyde Dehydrogenases by

https://doi.org/10.1021/acscentsci.1c00616
ACS Cent. Sci. 2021, 7, 1524−1534

Two Candidates for the Active Metabolites of Disulfiram. *Biochemistry* **1997**, *36* (44), 13748−13754.
(38) Weerapana, E.; Wang, C.; Simon, G. M.; Richter, F.; Khare, S.; Dillon, M. B.; Bachovchin, D. A.; Mowen, K.; Baker, D.; Cravatt, B. F. Quantitative reactivity profiling predicts functional cysteines in proteomes. *Nature* **2010**, *468* (7325), 790−5.
(39) Foster, C. E.; Bianchet, M. A.; Talalay, P.; Zhao, Q.; Amzel, L. M. Crystal structure of human quinone reductase type 2, a metalloflavoprotein. *Biochemistry* **1999**, *38* (31), 9881−6.
(40) Chen, Y.; Yang, Y.; Wang, F.; Wan, K.; Yamane, K.; Zhang, Y.; Lei, M. Crystal structure of human histone lysine-specific demethylase 1 (LSD1). *Proc. Natl. Acad. Sci. U. S. A.* **2006**, *103* (38), 13956−61.
(41) Toh, J. D. W.; Sun, L.; Lau, L. Z. M.; Tan, J.; Low, J. J. A.; Tang, C. W. Q.; Cheong, E. J. Y.; Tan, M. J. H.; Chen, Y.; Hong, W.; Gao, Y. G.; Woon, E. C. Y. A strategy based on nucleotide specificity leads to a subfamily-selective and cell-active inhibitor of N(6)-methyladenosine demethylase FTO. *Chem. Sci.* **2015**, *6* (1), 112−122.
(42) Morgan, C. A.; Parajuli, B.; Buchman, C. D.; Dria, K.; Hurley, T. D. N,N-diethylaminobenzaldehyde (DEAB) as a substrate and mechanism-based inhibitor for human ALDH isoenzymes. *Chem.-Biol. Interact.* **2015**, *234*, 18−28.
(43) Huang, Z.; Ogasawara, D.; Seneviratne, U. I.; Cognetta, A. B., 3rd; Am Ende, C. W.; Nason, D. M.; Lapham, K.; Litchfield, J.; Johnson, D. S.; Cravatt, B. F. Global Portrait of Protein Targets of Metabolites of the Neurotoxic Compound BIA 10−2474. *ACS Chem. Biol.* **2019**, *14* (2), 192−197.
(44) Mendoza, V. L.; Vachet, R. W. Probing protein structure by amino acid-specific covalent labeling and mass spectrometry. *Mass Spectrom. Rev.* **2009**, *28* (5), 785−815.
(45) Ringe, D.; Petsko, G. A.; Kerr, D. E.; Ortiz de Montellano, P. R. Reaction of myoglobin with phenylhydrazine: a molecular doorstop. *Biochemistry* **1984**, *23* (1), 2−4.
(46) Jonen, H. G.; Werringloer, J.; Prough, R. A.; Estabrook, R. W. The reaction of phenylhydrazine with microsomal cytochrome P-450. *J. Biol. Chem.* **1982**, *257* (8), 4404−11.
(47) Watanabe, K.; Ohkubo, H.; Niwa, H.; Tanikawa, N.; Koda, N.; Ito, S.; Ohmiya, Y. Essential 110Cys in active site of membrane-associated prostaglandin E synthase-2. *Biochem. Biophys. Res. Commun.* **2003**, *306* (2), 577−81.
(48) Yamada, T.; Takusagawa, F. PGH2 degradation pathway catalyzed by GSH-heme complex bound microsomal prostaglandin E2 synthase type 2: the first example of a dual-function enzyme. *Biochemistry* **2007**, *46* (28), 8414−24.
(49) Zhang, M.; Yang, S.; Nelakanti, R.; Zhao, W.; Liu, G.; Li, Z.; Liu, X.; Wu, T.; Xiao, A.; Li, H. Mammalian ALKBH1 serves as an N(6)-mA demethylase of unpairing DNA. *Cell Res.* **2020**, *30* (3), 197−210.
(50) George, T. P.; Weinberger, A. H. Monoamine oxidase inhibition for tobacco pharmacotherapy. *Clin. Pharmacol. Ther.* **2008**, *83* (4), 619−21.
(51) Golwyn, D. H. Cocaine abuse treated with phenelzine. *Int. J. Addict* **1988**, *23* (9), 897−905.
(52) Tort, S.; Urrutia, G.; Nishishinya, M. B.; Walitt, B. Monoamine oxidase inhibitors (MAOIs) for fibromyalgia syndrome. *Cochrane Database Syst. Rev.* **2012**, No. 4, CD009807.
(53) Davidson, J.; Raft, D. Monoamine oxidase inhibitors in patients with chronic pain. *Arch. Gen. Psychiatry* **1985**, *42* (6), 635−6.
(54) Mallinger, A. G.; Frank, E.; Thase, M. E.; Barwell, M. M.; Diazgranados, N.; Luckenbaugh, D. A.; Kupfer, D. J. Revisiting the effectiveness of standard antidepressants in bipolar disorder: are monoamine oxidase inhibitors superior? *Psychopharmacol Bull.* **2009**, *42* (2), 64−74.
(55) Volz, H. P.; Gleiter, C. H. Monoamine oxidase inhibitors. A perspective on their use in the elderly. *Drugs Aging* **1998**, *13* (5), 341−55.
(56) Mészáros, L.; Hoffmann, A.; Wihan, J.; Winkler, J. Current symptomatic and disease-modifying treatments in multiple system atrophy. *Int. J. Mol. Sci.* **2020**, *21* (8), 2775.

https://doi.org/10.1021/acscentsci.1c00616
ACS Cent. Sci. 2021, 7, 1524−1534